Eur. J. Wood Prod. (2013) 71:635–646
DOI 10.1007/s00107-013-0726-z

ORIGINALS ORIGINALARBEITEN

Prefabricated timber walls anchored with glued-in rod connections: racking tests and preliminary design

Gabriela Parida · Massimo Fragiacomo · Helena Johnsson

Received: 13 April 2011 / Published online: 29 July 2013

Abstract A new beam and post system for multi-storey timber buildings has been developed in Sweden. The building is braced with timber walls constructed from two Kerto-Q LVL boards glued and screwed onto a glulam frame. The walls are prefabricated off-site and can be connected to the foundation using either glued-in steel rods with metric thread or nail plates. Introductory racking tests of full scale walls anchored with glued-in threaded rods were performed. The paper presents the results of the experiments and discusses the use of the transformed section method to predict racking capacity of the anchored wall. To evaluate the strength of the glued-in rods, a newly proposed model was employed. An analytical study was conducted to investigate the role of the sheathing and the contribution of the axial force on the racking capacity of the walls. The wall panels tested in this experimental programme showed high strength and stiffness under racking load. The anchoring joints with glued-in steel rods with metric thread demonstrated a high load-carrying capacity with, however, large scatter and a brittle failure mode characterized by pull-out from the timber member. The transformed section method was successfully used to predict the racking capacity of timber walls anchored with glued-in steel rods.

G. Parida (✉) · H. Johnsson
Department of Civil, Environmental and Natural Resources Engineering, Luleå University of Technology, 971 87 Luleå, Sweden
e-mail: gabrielaparida@gmail.com

M. Fragiacomo
Department of Architecture, Design and Urban Planning, University of Sassari, 07041 Alghero, Italy

Mit eingeklebten Gewindestangen verankerte vorgefertigte Wandelemente - Wandscheibenprüfungen und vorläufige Bemessung

Zusammenfassung In Schweden wurde ein neues Ständerbausystem für mehrgeschossige Holzgebäude entwickelt. Das Gebäude ist mit Wandelementen ausgesteift, die aus einem Rahmen aus Brettschichtholz und zwei darauf verklebten und verschraubten Kerto-Q Furnierschichtholzplatten bestehen. Die vorgefertigten Wände können entweder mittels eingeklebter Gewindestangen mit metrischem Gewinde oder mit Nagelplatten auf dem Boden verankert werden. An originalgroßen Wänden, verankert mit eingeklebten Gewindestangen, wurden Wandscheibenversuche durchgeführt. In dieser Studie werden die Versuchsergebnisse vorgestellt und ein Modell zur Bestimmung der Tragfähigkeit von verankerten Wandscheiben diskutiert. Die Festigkeit der eingeklebten Gewindestangen wurde mit einem neu entwickelten Modell bestimmt. Der Beitrag der Beplankung und der axialen Kraft zur Wandscheibentragfähigkeit wurde in einer analytischen Studie untersucht. Die untersuchten Wandtafeln wiesen bei einer Wandscheibenbelastung eine hohe Festigkeit und Steifigkeit auf. Die Verankerung mit eingeklebten Stahlstangen mit metrischem Gewinde wies eine hohe Tragfähigkeit auf, jedoch mit großer Streuung und einem spröden Bruchverhalten, das durch Herausziehen der Gewindestangen aus dem Holz gekennzeichnet ist. Das entwickelte Modell erwies sich als erfolgreich zur Bestimmung der Wandscheibentragfähigkeit von Wandelementen, die mit eingeklebten Stahlgewindestangen verankert sind.

1 Introduction

The development of multi-storey timber construction is rapidly growing in Sweden. An innovative system with the Swedish commercial name "*träδ*" was recently developed by the Scandinavian glulam manufacturer Moelven Töreboda. In this system, a beam and post load-resisting structure made of glulam and Kerto LVL is braced with a new type of prefabricated wall panel placed at discrete locations in the floor (Tlustochowicz et al. 2010a). When resisting lateral loads, the timber walls act as vertical cantilevers transferring the lateral load applied to the building to its foundation. The structural system offers large flexibility in architectural design and the possibility to have large windows along the façade and open spaces (Fig. 1).

The timber walls used in the *träδ* system are elements with a high aspect (height/width) ratio (2.5–6.5). High aspect ratios are unfavourable for light shear walls as their stiffness and strength are greatly reduced (Salenikovich and Dolan 2003). However, the stiffness of slender walls can be significantly improved by gluing the sheathing to the frame as demonstrated for example by Filiatrault and Foschi (1991). The wall elements are prefabricated as composite panels comprising Kerto-Q LVL sheathings glued onto a glulam frame, with cross-bonded veneers in the lateral direction (Fig. 2). Screws are used only to apply pressure during the bonding process.

The wall panels are typically 2.4 m wide due to limitations in LVL production and transportation and can be continuous up to a height of four storeys, which is considered the upper limit for transportation. Anchoring by glued-in steel metric rods was chosen since it has been successfully used in Sweden for anchoring vertical members (Carling 2001) and also for its potentially high stiffness and pull-out strength capacity. The glued-in threaded rods connect the wall to a steel profile which is anchored to the foundation. To make the assembly of the slender wall elements easier, the panels can be combined into T-shaped configurations (Fig. 1), which allows them to be self-stabilising during erection.

This paper presents the results of a series of full-scale racking tests with the main objective to evaluate the performance of the prefabricated wall panels subjected to lateral load and their glued-in anchorage system. Provisions for the design of the timber walls and anchorages are also provided.

2 Experimental set-up

2.1 Wall panels

Three wall panels were subjected to monotonic racking tests. Full-scale specimens were used; however, due to space limitations in the laboratory, the height of the wall panels was taken as 6 m, which is half the height of a four storey building. The elevation of the wall element and its cross-section are displayed in Fig. 2 and the view of the experimental set-up in Fig. 3. The frame was made of Swedish glulam of strength class L40 (corresponding to strength class GL28c according to EN 1194 1999). Three continuous vertical glulam members of the frame were connected to the horizontal members placed in between by means of LVL sheathing on both sides. The cross-section of the outer vertical framing members was 160 × 360 mm^2, the intermediate one 160 × 225 mm^2, and the horizontal members 160 × 225 mm^2 (Fig. 2).

No joints were assembled between the vertical and horizontal members. The LVL sheathing was 27 mm thick Kerto-Q boards, where 20 % of the veneers have crosswise direction. The sheathing was glued and screwed to the

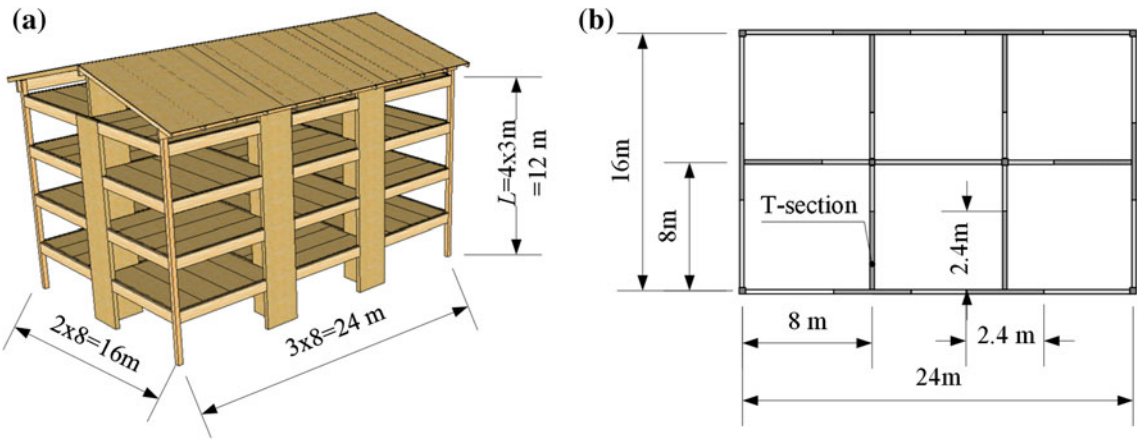

Fig. 1 3D view (**a**) and plan (**b**) of the post and beam system träδ used in a case study multi-storey building [dimensions in mm]
Abb. 1 **a** 3D-Ansicht und **b** Grundriss des mehrgeschossigen Ständerbausystems träδ, das in einer Fallstudie verwendet wurde (Abmessungen in mm)

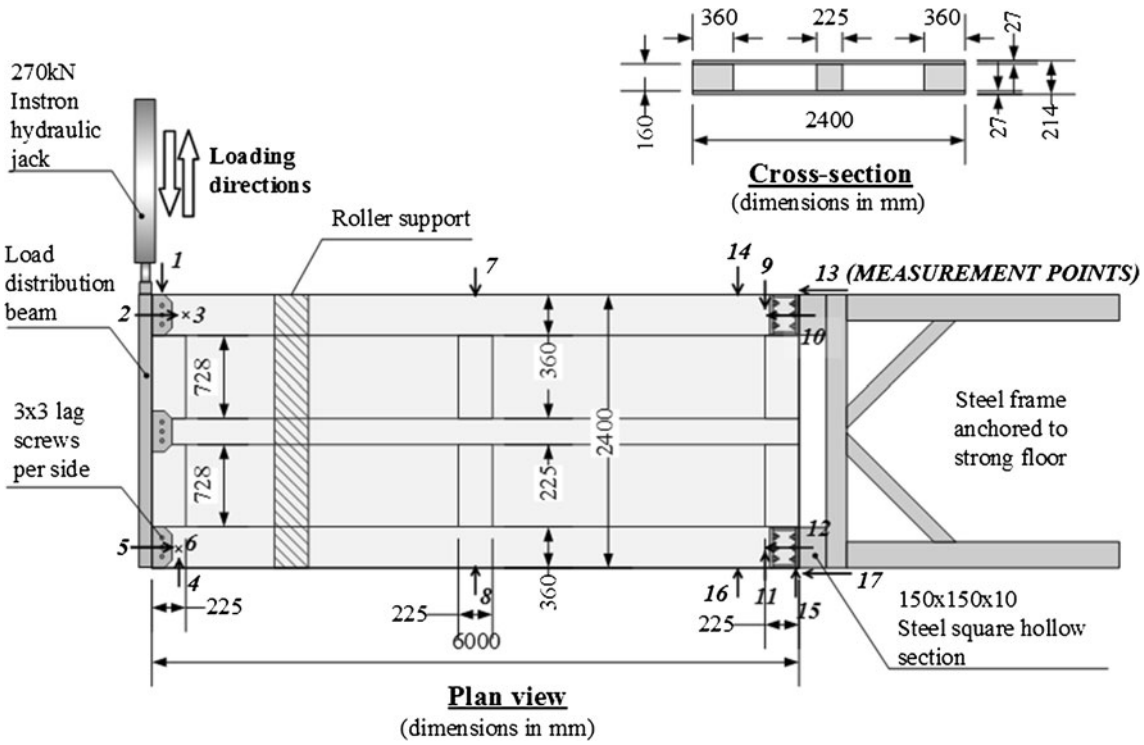

Fig. 2 Test set-up (transducers are indicated with *arrows*) [dimensions in mm]
Abb. 2 Versuchsaufbau (Wegaufnehmer sind mit Pfeilen markiert) (Abmessungen in mm)

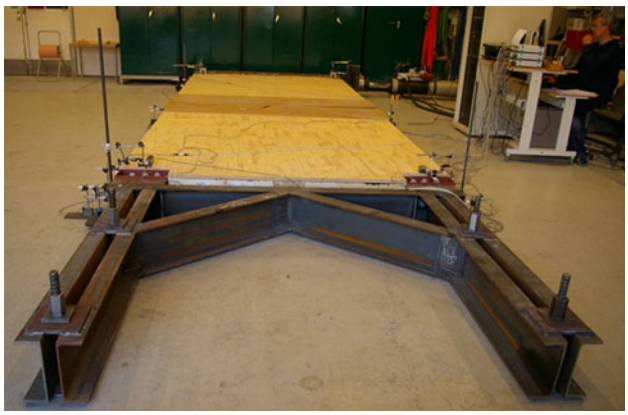

Fig. 3 View of the experimental set-up
Abb. 3 Aufnahme des Versuchsaufbaus

framing members on both sides using Resorcinol Casco base 1719 hardener 2619 adhesive, and Heco TFT Protect 4 6.0 × 80 screws, with a spacing of approximately 300 mm centre to centre. The specimens were produced in the glulam factory of Moelven Töreboda, Sweden. The moisture content and density of the materials during testing were determined according to recommendations in ISO 3130: 1975 and ISO 3131: 1975, respectively. For glulam the mean density was determined to 479 kg/m^3 at a mean moisture content of 12.8 %. For LVL the mean density was 487 kg/m^3 and the mean moisture content 10.6 %. More details of the experimental study can be found in Tlustochowicz (2010).

The design lateral load was based on the most unfavourable wind load case in Sweden (sum of the pressure on the windward and leeward facades of 1.29 kN/m^2) applied to the entire case study building displayed in Fig. 1 (Tlustochowicz 2011). The calculation was based on the Swedish design code (BKR 1998). The design bending moment at the foundation was calculated as $M_{1,\mathrm{Ed}} = 395$ kNm (see Fig. 4a), which corresponds to a characteristic bending moment $M_{1,\mathrm{Ek}} = 290$ kNm when no partial factors for actions are considered. In this calculation, the racking forces $F_{\mathrm{v},1,\mathrm{Ed}}$, $F_{\mathrm{v},2,\mathrm{Ed}}$, $F_{\mathrm{v},3,\mathrm{Ed}}$ and $F_{\mathrm{v},4,\mathrm{Ed}}$, at each floor are equal to 8.3, 16.7, 16.7 and 10 kN, respectively.

2.2 Anchorage

Two anchoring connections were used at each lower corner. The connection consists of 6ø24 metric threaded rods, class 8.8 [$f_y = 640$ N/mm^2, $f_u = 800$ N/mm^2 in accordance with Eurocode 3 (EN 1993-1-1: 2005)]. The set-up of the connection was proposed by the manufacturer and the glued-in lengths were calculated according to DIN 1052:2008-12 Entwurf (2008) and Steiger et al. (2007). The edge distances as well as the rod spacing were chosen as suggested by Serrano (2001).

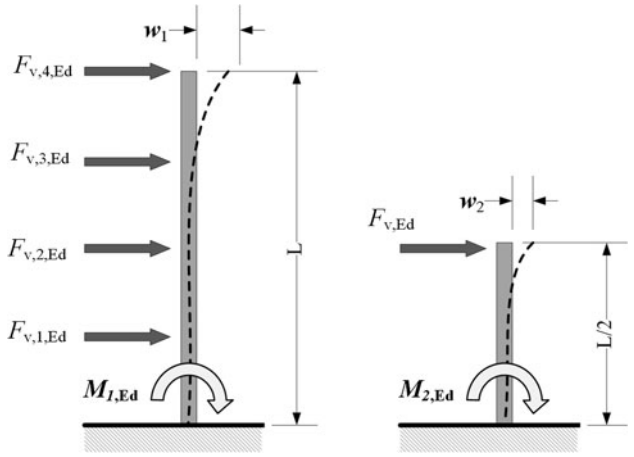

Fig. 4 Illustration of calculation of scale factor: **a** design case, **b** experiment
Abb. 4 Darstellung der Berechnung des Maßstabsfaktors: **a** Bemessung, **b** Versuch

The glued-in length of rods was calculated as $l_a = 300$ mm (Fig. 5). The holes drilled in the glulam were 1 mm larger than the diameter of the rods (resulting in a glueline thickness of 0.5 mm) and had a length of 310 mm. The adhesive used was two-component polyurethane, Purbond CR 421. During production, the adhesive mixed with hardener was injected into the hole; thereafter the rod was inserted into the hole simultaneously pressing out the adhesive and distributing it along the rod. The procedure followed the recommendation given by the national type approval (Typgodkännandebevis 1396/78: 2009).

To enable connection of the threaded metric rods to the foundation, a HEB 180 steel profile was used as an intermediate connector (Fig. 5). The rods glued into glulam, as well as the rods cast in the concrete foundation, were fastened to the flanges of the steel part by nuts and washers. To decrease the deformation of the flanges, 10 mm thick stiffening plates were welded on both ends of the steel part.

2.3 Test set-up

The test was performed with the wall panel in a horizontal position and supported by a roller placed at approximately two thirds of the height (Fig. 2). The actual connection of the HEB 180 steel part to the foundation was simulated in the tests by connecting the profile to a steel frame via a steel square hollow section (Fig. 2). The steel frame was screwed and welded to the floor.

The specimens were instrumented with 17 Linear Voltage Displacement Transducers (LVDTs) with a measurement length between 10 and 100 mm (Fig. 2) (marked as measurement points). Out-of plane displacements were measured at the top corners of the specimen by LVDTs No. 3 and 6.

The influence of self-weight, which in a real situation would partially counteract the uplift of the structure (Vessby 2008; Filiatrault and Foschi 1991), was conservatively neglected. The racking load was applied at the top of the wall element through a hydraulic jack with a displacement range of ±400 mm and a capacity of 270 kN. The jack was then connected to a load distributing steel beam screwed to the framing members at the top of the wall panel from both sides. Due to some limitations in the laboratory facilities, the end of the hydraulic jack was fixed to the end of the load distributing beam thereby restraining somewhat the free rotation of the wall during loading and therefore reducing the deflection on top of the wall compared to a wall fully unrestrained.

Each specimen was subjected to the racking test in two directions (Fig. 2). The load was first increased

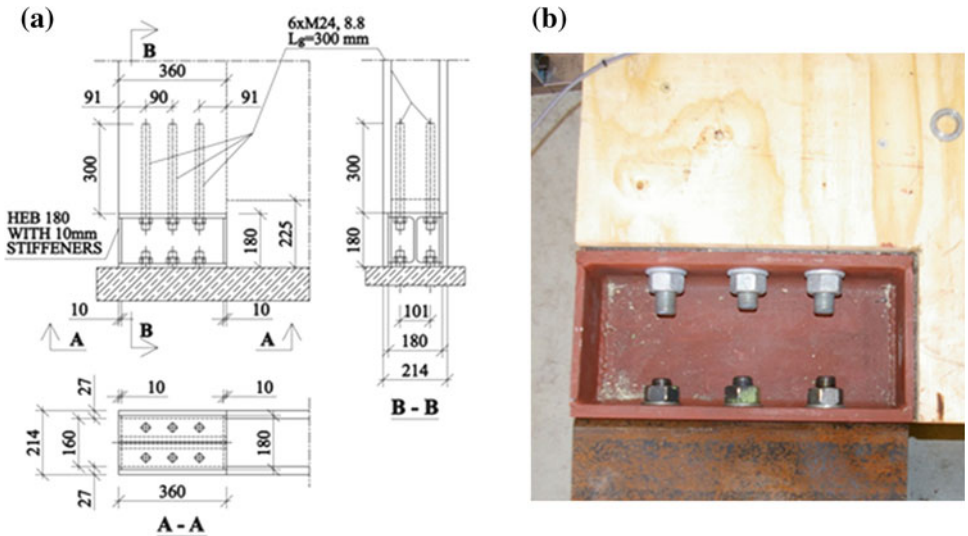

Fig. 5 Detail (**a**) and photo (**b**) of the anchorage device with glued-in rods [dimensions in mm]
Abb. 5 **a** Detail und **b** Aufnahme der Verankerung mit eingeklebten Gewindestangen (Abmessungen in mm)

monotonically in one direction up to failure of the connection loaded in tension. The specimen was then unloaded and reloaded monotonically in the opposite direction up to failure of the other hold-down connection. The first specimen was subjected to several preliminary loading–unloading cycles before the final load–displacement curve was recorded.

3 Test results

3.1 Load–displacement curves

The load–displacement curves obtained for the top end of the wall (measurement point 1) panels are presented in Fig. 6. The first number in the designation of the curves (1, 2 and 3) represents the specimen number, and the second one stands for the connection (R-right, L-left) loaded in tension. The lateral displacements obtained in the racking test are a sum of three components: shear, bending and rocking of the panel (Vessby 2008; Tlustochowicz et al. 2010b). Due to the insufficient stiffness and strength of the steel frame simulating the foundation, additional unintended deflection components occurred from rotation and translation of the steel frame itself. Such components, measured during experiment, were subtracted from the total deflection recorded (Tlustochowicz et al. 2010b; Tlustochowicz 2010). The results presented in Fig. 6 therefore include only the displacement components that occurred in the wall panels and in the anchoring hold-downs.

It was observed that the tested walls have a large initial stiffness with an average value of 6.9 kN/mm. The specimens exhibited a close to linear behaviour with the only visible nonlinearity occurring just prior to failure, which in one case (test T-2R, Fig. 6) was caused by local deformations of the upper flange of the HEB profile.

3.2 Racking load resistance

All tested elements performed well under lateral loading demonstrating no significant damage. Their racking resistance was determined as the maximum horizontal load reached before any visible decrease in load on the load–displacement diagram occurred, which corresponds to a failure in the connection. The experimental racking resistance of the prefabricated wall panels $F_{v,R}$ varied between 98.3 and 214 kN (on average 157 kN) (Table 1). The design value of the total racking load, calculated according to the Swedish design code accounting for wind load on a 4-storey case study building (as displayed in Fig. 1), was $F_{v,Ed} = 65.8$ kN. In the following, subscripts 'R' and 'E' are used to denote the resistance and the effect of the load, respectively, in accordance with Eurocode 5 (EN 1995-1-1: 2004) notations.

3.3 Failure

Generally, the observed failure mode in all cases was brittle, caused by pull-out failure of the rods, which was due to shear around the rods, either along the surface of the

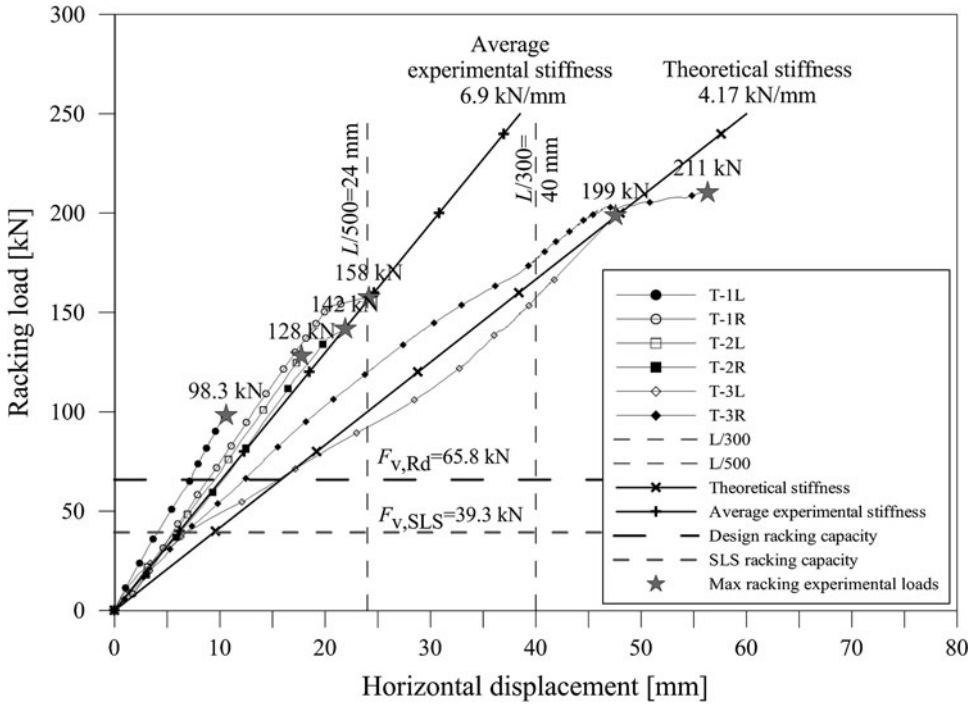

Fig. 6 Load-top lateral displacement curves
Abb. 6 Kraft-Weg-Diagramme mit Lasteinleitungsbereich

Table 1 Summary of the step-by-step analysis for the prediction of the load-carrying capacity of the wall, and comparison with experimental results
Tabelle 1 Zusammenfassung der schrittweisen Analyse zur Bestimmung der Tragfähigkeit der Wand und Vergleich mit Versuchsergebnissen

Case	Sum of glued-in lengths (mm)	Experimental racking strength $F_{v,R,exp}$ (kN)	Predicted mean racking strength					
			Case 1a		Case 1b		Case 1c	
			$F_{v,Rmean,1a}$ (kN)	Difference (%)	$F_{v,Rmean,1b}$ (kN)	Difference (%)	$F_{v,Rmean,1c}$ (kN)	Difference (%)
Ideal situation	1,800	–	223	$(F_{v,Rmean,1a}-F_{v,R,exp})/F_{v,R,exp}$	240	$(F_{v,Rmean,1b}-F_{v,R,exp})/F_{v,R,exp}$	341	$(F_{v,Rmean,1c}-F_{v,R,exp})/F_{v,R,exp}$
1L	830	98.3	75.1	−23.6	75	−23.7	81.4	−17.1
1R	1,365	158	134	−15.2	134	−15.1	139	−11.8
2R	1,460	142	147	3.7	147	3.5	146	2.7
2L	1,300	128	124	−3.5	124	−3.4	126	−1.9
3R	1,225	214	122	−42.9	122	−43.0	113	−47.4
3L	1,770	199	216	8.4	216	8.6	224	12.4
Average value		157	136	−12.2	136	−12.2	138	−10.5

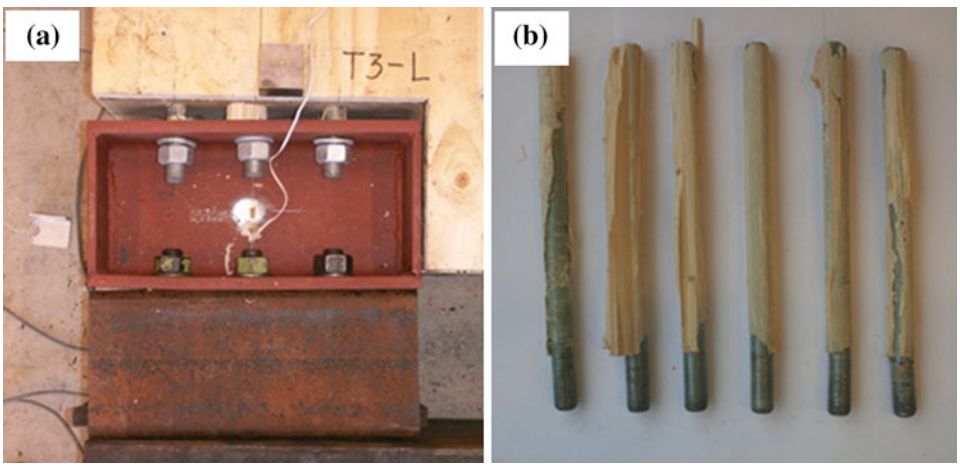

Fig. 7 Failure in the connection (**a**), evaluation of glued-in lengths in connection 2R (**b**)
Abb. 7 **a** Bruch in der Verbindung, **b** Bestimmung der Einklebelängen der Verbindung 2R

adhesive (Fig. 7a) or in the timber as shear plugs. In test No. 3R, where the highest failure load was obtained, the glued-in rod joint did not fail before the maximum load capacity of the jack was reached. Examination of the individual pulled-out rods after the experimental tests revealed that the rods in the connections were not glued along their entire length. The effective adhesive area was estimated to 46–88 %, see for example Fig. 7b, which is the most probable reason for the large scatter of the experimental results.

4 Analytical models

4.1 Prediction of the elastic lateral displacements

In the design of the experiment, a 4-storey high timber wall was considered loaded with four horizontal forces $F_{v1,Ed}$, $F_{v,2,Ed}$, $F_{v3,Ed}$ and $F_{v,4,Ed}$ placed accordingly at heights x_1, x_2, x_3 and x_4 corresponding to the locations of floor beams (Fig. 4a).

In this case, the maximum lateral deflection caused by shear and bending of the wall (w_1) can be calculated as a sum of deflection contributions of the different loads to the cantilever beam, Eq. 1:

$$w_1 = w_{1,shear} + w_{1,bend} = \beta \sum_{i=1}^{4} \frac{F_{v,i,Ek} \cdot x_i}{GA_{tr}} + \sum_{i=1}^{4} \frac{F_{v,i,Ek} \cdot x_i^2 \cdot (3L - x_i)}{6EI_{tr}} \quad (1)$$

where $L = 12$ m is the height of the wall, $\beta = 2.54$ is the shear factor calculated for the cross-section of the wall using the formulas of solid mechanics for beams subjected to shear (see full derivation in Tlustochowicz 2011), and GA_{tr} and EI_{tr} are calculated for the composite cross-section of the wall. The predicted maximum lateral displacement of the top floor at serviceability limit state (SLS) due to the loads $F_{v,i,Ed}$ applied at each floor 'i' was $w_1 = 9.8$ mm. In

the experimental case the wall element had a reduced height of $L/2$ (Fig. 4b) and the applied lateral load $F_{v,Ed}$ was calculated so as to induce the same bending moment at the base of the wall as the load system $F_{v,1,Ed}$, $F_{v,2,Ed}$, $F_{v,3,Ed}$, and $F_{v,4,Ed}$. The theoretical maximum lateral displacement (w_2) is:

$$w_2 = w_{2,shear} + w_{2,bend} = \beta \frac{F_{v,Ed} \cdot (L/2)}{GA_{tr}} + \frac{F_{v,Ed} \cdot (L/2)^3}{3EI_{tr}} \quad (2)$$

The predicted displacement at SLS was $w_2 = 8.7$ mm. By assuming a typical range of variation of E and G with respect to their mean value of Coefficient of Variation, corresponding to 12 % (Sousa et al. 2013), the predicted deflection w_2 varies from 7.8 to 9.9 mm. To represent the displacement of a full height wall loaded with a system of four loads $F_{v,1,Ed}$, $F_{v,2,Ed}$, $F_{v,3,Ed}$, $F_{v,4,Ed}$ (Fig. 4a), the experimental results on the reduced height wall had to be multiplied by a scale factor: $w_1/w_2 = 9.8/8.7. = 1.13$ (Fig. 4b).

The scaled displacements at the experimental failure load varied between 8.4 and 45 mm (21.1 mm on average). At 40 % of the minimum experimental racking strength, corresponding to the SLS load level of 39.3 kN, the deflection lays in the range between 4.1 and 6.9 mm (5.9 mm on average), which multiplied by the scale factor 1.13 leads to 4.6–7.8 mm (6.7 mm on average). This is below the recommended limits of $L/500$ or $L/300$ (Källsner and Girhammar 2008) corresponding to 24 and 40 mm, respectively. By comparing the variation of the experimental and analytical values of deflection, it can be noted that the total variation of experimentally obtained displacements exceeded the variation caused by probable variation in material properties. It is likely that the use of multiple materials with inhomogeneous properties plays a significant role in obtaining large scatter of experimental results.

The significant difference in Fig. 6 between analytical and experimental stiffness of the panel is most likely due to the additional restraint of the top end of the cantilever wall provided by the hydraulic jack that had to be fixed to the load distributing beam due to some limitations in laboratory facilities.

4.2 Glued-in rods

As a consequence of the lack of general consensus on the analytical modelling of glued-in rod connections, no recommendations can be found in Eurocode 5 (1995-1-1). One of the latest proposals, applicable to the tested configuration, was chosen to carry out a theoretical analysis and compare the mean experimental and analytical pull-out strengths $F_{ax,R,mean}$ of the rods to provide a design method for the timber walls.

The model used was developed by Aicher et al. (1999), Eq. 3.

$$F_{ax,R,mean} = \pi \cdot d_h \cdot l_a \cdot f_{v,mean} \quad (3)$$

where $F_{ax,R,mean}$, d_h, l_a and $f_{v,mean}$ signify the mean pull-out strength of the rod in [N], the diameter of the hole in [mm], the glued-in length in [mm], and the mean shear strength of the bond in [N/mm^2]. The shear strength is given by Eq. 4:

$$f_{v,mean} = \min\left\{ 8\frac{N}{mm^2}; 129 \cdot d^{-0.52} \cdot \lambda^{-0.62} \cdot \left(\frac{\rho}{480}\right)^{0.45} \right\} \quad - \text{ for PUR adhesive} \quad (4)$$

where d, λ, and ρ are the diameter of the rod in [mm], the slenderness of the rod ($\lambda = l_a/d$ [−]), and the density of the glulam in [kg/m^3] respectively. According to this model, the calculated mean shear strength of the bond $f_{v,mean}$ is 5.16 N/mm^2 (using the average experimental density of 479 kg/m^3), as evaluated in Tlustochowicz (2010), and the mean analytical pull-out strength of one rod fully glued along its length is $F_{ax,R,mean} = 119$ kN.

4.3 Wall-foundation connection

4.3.1 Stress distribution

The analysed walls are composite elements built from two different wood engineered materials connected to each other by means of both mechanical connectors and adhesive. The mechanical connectors are used to apply the pressure during curing of the adhesive and do not contribute to the strength and stiffness of the connection. Thus, the cross-section of the wall can be considered as rigid. Based on the approach proposed by Batchelar (2006) and Fragiacomo and Batchelar (2012) for the design of timber moment connections with glued-in rods, the transformed section method was employed to analyse the stress distribution at the wall-foundation interface (Fig. 8). This approach uses the assumptions of plane sections remaining plane and linear stress distribution in the compressed timber area. The lateral force ($F_{v,E}$) applied to the top corner of the wall element causes a bending moment (M_E) at the wall-foundation interface, thus one of the anchorage joints is subjected to tension and the other one to compression. Six steel rods are the active section resisting the tensile force ($F_{t,E}$), while in the opposite connection timber resists compression ($F_{c,E}$) by direct contact (bearing) to the steel part and from this to the foundation (Fig. 7).

The specimens were manufactured so that during the experiment the Kerto sheathing had no contact with the HEB 180 steel part, thus only glulam rested on the foundation and participated in the transfer of compression force.

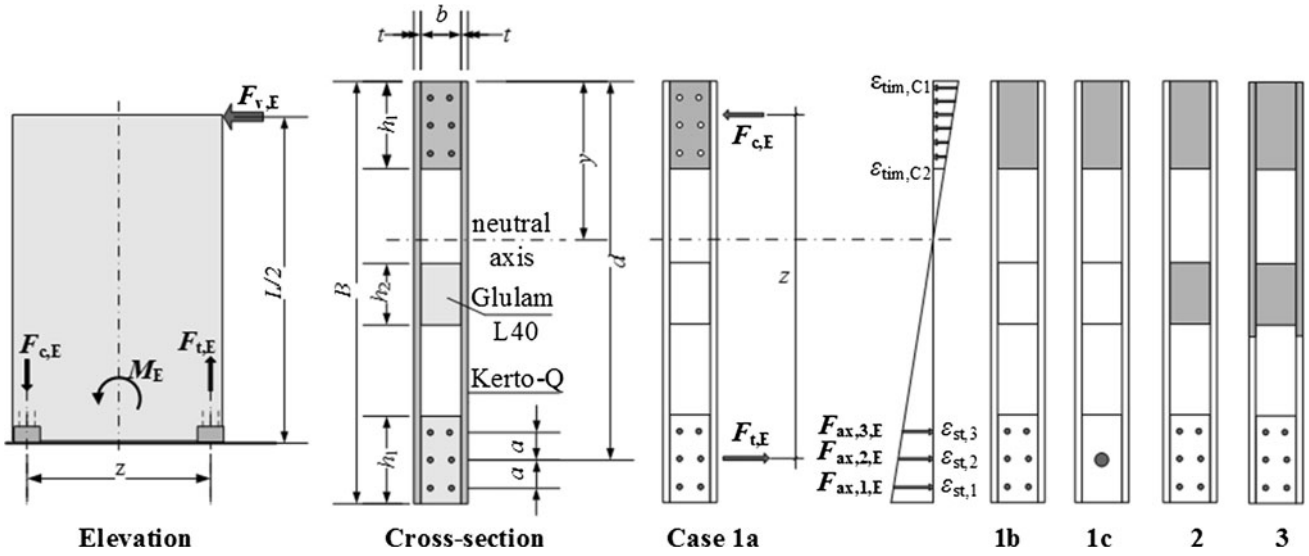

Fig. 8 Transformed section method for stress analysis at the wall-foundation interface—*grey* areas denote the resisting parts of the cross-sections
Abb. 8 Modell zur Spannungsanalyse des Kontaktbereichs von Wand und Boden – die grauen Flächen zeigen die einwirkenden Querschnittsbereiche

Also the part of the specimen between the anchorage devices (along the distance z-h_1) was entirely unsupported. The glued-in rods in the compression area were not considered in the analysis as they were not welded to the HEB 180 steel profile and, hence, could not carry any compression force. The theoretical analysis was performed with different assumptions. In case 1a of Fig. 8, the areas of holes ($6A_h$) in the glulam member were subtracted from the compression area, whereas in case 1b the whole cross-section of the glulam member was taken as the compression area. On the tension side, for both cases, each pair of glued-in rods with cross-sectional area A_s was considered as one layer of reinforcement, which gives different tensile forces in each pair with the assumption of a linear stress distribution. In the ideal case, when the rods are fully glued along their length l_a (6×300 mm $= 1{,}800$ mm), the failure of the outermost pair implies failure of the entire connection. In case 1c, the group of rods was concentrated in the centroid of the actual connection.

The compression force ($F_{c,E}$) and tension force ($F_{t,E}$) are given by:

$$F_{c,E} = \sigma_{tim,C2} h_1 + \frac{1}{2}(\sigma_{tim,C1} - \sigma_{tim,C2}) h_1 \tag{5}$$

$$F_{t,E} = 2A_s\sigma_{st,1} + 2A_s\sigma_{st,2} + 2A_s\sigma_{st,3} \tag{6}$$

where $\sigma_{tim,C1}$ and $\sigma_{tim,C2}$ represent the stresses in the external fibres of the compressed timber section with height of h_1; $\sigma_{st,1}$, $\sigma_{st,2}$ and $\sigma_{st,3}$ are the tensile stresses in pairs of steel rods.

The position of the neutral axis (y) can be determined by imposing the condition of zero first moment of area of the resisting transformed section about the neutral axis, which for case 1a leads to Eq. 7:

$$\begin{aligned} S_{x,1a} = {} & h_1 \cdot b \cdot \left(y - \frac{h_1}{2}\right) - \left[2 \cdot A_h \cdot \left(y - \frac{h_1}{2} + a\right)\right. \\ & + 2 \cdot A_h \cdot \left(y - \frac{h_1}{2}\right) + 2 \cdot A_h \cdot \left(y - \frac{h_1}{2} - a\right)\Big] \\ & - [2 \cdot A_s \cdot n \cdot (d - y + a) + 2 \cdot A_s \cdot n \cdot (d - y) \\ & + 2 \cdot A_s \cdot (d - y - a)] = 0 \end{aligned} \tag{7}$$

The geometrical representations of symbols h_1, b, h_2, a, d, and y are illustrated in Fig. 8. Symbol n represents the steel-to-timber modular ratio ($n = E_s/E_t$, where E_s and E_t are the Young's modulus of the steel rods and glulam member, respectively). Once the quantity y is known, the second moment of area of the resisting transformed area about the neutral axis (I_x) can be calculated:

$$\begin{aligned} I_{x,1a} = {} & \frac{bh_1^3}{12} + bh_1\left(y - \frac{h_1}{2}\right)^2 - 2A_h\left(y - \frac{h_1}{2}\right)^2 \\ & - 2A_h\left(y + a - \frac{h_1}{2}\right)^2 - 2A_h\left(y - a - \frac{h_1}{2}\right)^2 \\ & + 2 \cdot n \cdot A_s(d + a - y)^2 + 2 \cdot n \cdot A_s(d - y)^2 \\ & + 2 \cdot n \cdot A_s(d - a - y)^2 \end{aligned} \tag{8}$$

and the stresses in the cross-section are given by:

$$\sigma_{tim,C1} = -\frac{M_{Ed}}{I_x} y \tag{9}$$

$$\sigma_{tim,C2} = -\frac{M_{Ed}}{I_x}(y - h_1) \tag{10}$$

$$\sigma_{st,1} = n\frac{M_{Ed}}{I_x}(d - y + a) \quad (11)$$

$$\sigma_{st,2} = n\frac{M_{Ed}}{I_x}(d - y) \quad (12)$$

$$\sigma_{st,3} = n\frac{M_{Ed}}{I_x}(d - y - a) \quad (13)$$

For case 1b, the area of the holes (A_h) can be assumed zero. For case 1c, zero distance between the rods is assumed, namely $a = 0$.

Based on the actual glued-in lengths (measured at the end of the test), a 'step-by-step' analysis of each joint was performed in order to theoretically model the failure mechanism and the corresponding failure load. By assuming a linear stress distribution in the connection, the forces in all rods $F_{\mathrm{ax,i,E}}$ can be calculated as functions of the applied racking load $F_{v,E}$.

$$\forall i \in (1..6) \Rightarrow F_{ax,i,E} = \sigma_{st,i}A_{st} \quad (14)$$

$$\text{e.g. } F_{ax,1,E} = \frac{F_{v,E} \cdot L \cdot A_s \cdot n \cdot (d - y + a)}{I_{x0}}, \text{ etc.} \quad (15)$$

By equating the forces in the rods $F_{\mathrm{ax,i,E}}$ and the mean pull-out strengths $F_{\mathrm{ax,Rmean}}$ calculated according to Eq. 3, it is possible to calculate the mean load-carrying capacity under lateral load (racking resistance):

$$F_{ax,Rmean} - F_{ax,i,E} = 0 \Rightarrow F_{v,Rmean,1} \quad (16)$$

Through Eq. 16, the mean applied racking load causing the failure of the weakest rod in the connection is obtained ($F_{\mathrm{v,Rmean,1}}$). After failure of the first rod, the load is redistributed between the remaining rods and a new, reduced second moment of area of the transformed resisting section can be calculated (I_{x2}). Following the same procedure as described above, in each step the racking load causing the failure of the consecutively weaker rods can be calculated ($F_{\mathrm{v,Rmean,i}}$). The analysis is completed when $F_{\mathrm{v,Rmean,i+1}} < F_{\mathrm{v,Rmean,i}}$, which indicates progressive failure of all remaining rods in the connection.

In Table 1 the results of the step-by-step analysis are expressed as the horizontal/racking load causing failure in the anchorage subjected to tension. The method proposed by Aicher et al. 1999 (Eqs. 3–4) was used to predict the pull-out strength capacity of the glued-in rods.

The results presented in Table 1 indicate that the method proposed by Aicher et al. (1999) shows good agreement with the experimental values. The analysis also illustrates that the results for cases 1a and 1b are almost identical, which implies that the area of the holes in the compression zone can be neglected. It can also be observed that when the rods are not fully glued along their length, a more detailed analysis (cases 1a and 1b) is recommended as the use of the simplified approach (1c) slightly overestimates the load-carrying capacity of the system.

4.3.2 Contribution of axial force

In the experimental programme, no axial force (representing self-weight and the service loads from different storeys) was applied to the wall specimen. In reality, these compression forces counteract the overturning moment caused by the wind load. Therefore it is of interest to investigate analytically the significance of this stabilising effect.

The transformed section method was used again to plot the axial load—bending moment interaction domain as presented in Fig. 9. The analytical procedure followed to plot the limit domain is similar to that used for reinforced concrete sections: (i) a position of the neutral axis y is assumed (Fig. 8); (ii) the attainment of the limit stress of timber in compression parallel to the grain $\sigma_{\mathrm{tim,C1}}$ is considered in the top fibre of the section; (iii) based on Bernoulli's hypothesis, the force in the lower rod $F_{\mathrm{ax,1,E}}$ is calculated from congruence and compared to the pullout strength $F_{\mathrm{ax,1,Rmean}}$; (iv) if $F_{\mathrm{ax,1,E}}$ is greater than $F_{\mathrm{ax,1,Rmean}}$, the failure mechanism will be rod pull-out, $F_{\mathrm{ax,1,E}}$ is assumed equal to $F_{\mathrm{ax,1,Rmean}}$, and the stress $\sigma_{\mathrm{tim,C1}}$ has to be recalculated from congruence; (v) the resultant axial force N_R and bending moment resistance M_R are then evaluated using equilibrium equations; (vi) the position of the neutral axis y is varied to minus and plus infinity and the procedure (i)–(v) is repeated by calculating the corresponding axial forces $N_R(y)$ and bending moment $M_R(y)$. The obtained experimental mean racking moment capacity of the wall is $M_{\mathrm{Rmean}} = 939$ kNm when no axial force is applied ($N_{\mathrm{Rmean}} = 0$). The mean bending moment resistance of the wall can be increased up to 1,988 kNm (112 % more) when an axial compression force $N_{\mathrm{Rmean}} = 743$ kN is applied (mean values in Fig. 9a). The maximum design bending moment resistance is $M_{\mathrm{Rd}} = 1{,}279$ kNm when a design compression force $N_{\mathrm{Rd}} = 710$ kN is applied. Note that the mean experimental bending moment resistance $M_{R,exp} = 939$ kNm in the absence of compression load lays in between the mean and design analytical bending moment resistance values.

4.3.3 Contribution of the middle framing member and sheathing

From a design perspective, it is interesting to explore how much the middle glulam member of the framing can contribute to the load-carrying capacity of the wall element if the wall was produced so that there was contact between the middle glulam member and the foundation (case 2

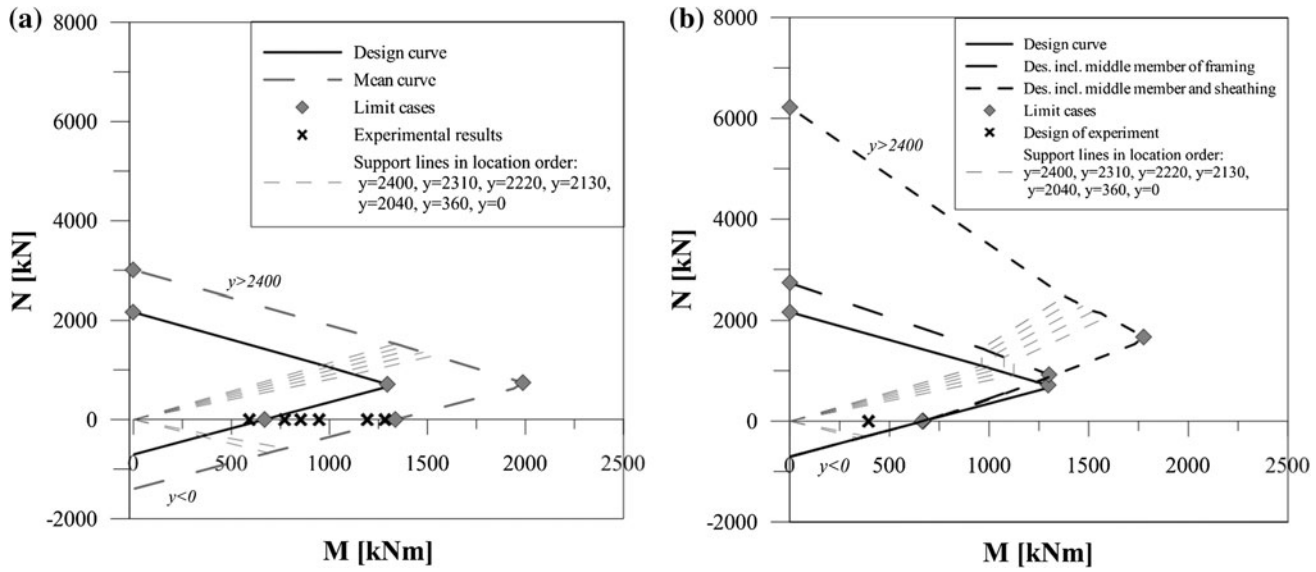

Fig. 9 Bending moment-axial load interaction diagram: **a** corresponding to case 1b in Fig. 8 and **b** corresponding to cases 1b, 2 and 3
Abb. 9 Interaktionsdiagramm von Biegemoment und Horizontallast: **a** entspricht Fall 1b in Abb. 8; **b** entspricht den Fällen 1b, 2 und 3 in Abb. 8

Table 2 Comparison of different theoretical approaches
Tabelle 2 Vergleich der verschiedenen theoretischen Ansätze

Case	Pure bending		Pure compression		Max resistance	
	M_R (kNm)	N_R (kN)	M_R (kNm)	N_R (kN)	M_R (kNm)	N_R (kN)
Mean values, case 1b	1,337	0	0	3,005	1,988	725
Design values, case 1b	669	0	0	2,164	1,297	710
Design values, case 2	667	0	0	2,730	1,299	926
Design values, case 3	664	0	0	6,215	1,775	1,677

illustrated in Fig. 8). Further, it is also interesting to investigate the effect of contact between the steel part and the LVL sheathing and contact between the sheathing and the foundation (case 3, Fig. 8). The transformed section method was employed to examine these two cases.

In Table 2 and in Fig. 9b, results of the theoretical analysis are presented for case 1b, which is more accurate than case 1c as it considers the actual distribution of the glued-in rods over the cross-section (see Table 1), case 2 and case 3 (as illustrated in Fig. 8) as an axial force—bending moment design domain. In the analysis, when the pull-out strength of the rod was decisive for the failure, Eq. 3 was used to determine its value. Results presented in Table 2 and Fig. 9b show that the contribution of the middle framing member can increase the compression capacity of the wall of approximately 26 % in comparison to the basic design case (1b). Taking into account the sheathing increases significantly the total racking capacity of the wall and the maximum design resistance that can be achieved is the point $M_{max,Rd} = 1{,}775$ kNm, $N_{max,Rd} = 1{,}677$ kN. A careful manufacturing process to ensure the contribution of all components of the wall to the load-carrying capacity can therefore be worthwhile.

5 Conclusion and discussion

5.1 Wall element

Results of monotonic static racking tests on a special timber wall panel connected to foundation with glued-in steel rods with metric thread have been presented. The minimum racking resistance obtained in the experimental programme was $F_{v,R} = 98.3$ kN (moment resistance $M_R = 590$ kNm), which exceeded the design value for a 4-storey case study building ($M_{Ed} = 395$ kNm). The moment capacity of the wall can be significantly increased if the positive effect of the vertical loads acting on the system (permanent and imposed loads of the floors) is taken into account. The highest design resistance that could be achieved in this case is $M_{Rd} = 1{,}297$ kNm for an axial load $N_{Rd} = 710$ kN, which

leaves a margin for increasing the height of the case study building.

5.2 Design method

In this paper a method for predicting the strength and lateral stiffness of timber wall elements anchored with glued-in rods was proposed, which is based on the transformed section method to calculate the stress distribution at the wall-foundation interface. Formulas for the pull-out strength of the hold downs made of a group of glued-in rods were applied. The predicted value of the average racking strength ($F_{v,Rmean} = 136$ kN) fairly underestimated the racking strength of the wall in comparison to the average experimental results ($F_{v,R,exp} = 156$ kN), whilst a more significant error was found in the lateral stiffness, with the analytical value (4.17 kN/mm) being conservative compared to the experimental value (6.9 kN/mm).

In order to use the proposed timber walls for the beam and post system *trä8*, a detailed study should be conducted to develop a design of the anchorage that exhibits a more ductile behaviour. One of the possible design improvements could be to detail the anchoring connection such that the steel rod is the weakest link in the connection and, therefore, the failure occurs with a yielded rod. This can be achieved by using a softer/milder steel (e.g. Gattesco and Gubana 2006), by using several rods with a smaller diameter instead of few large diameter rods (e.g. Baroth et al. 2004), or by reducing the cross-section of the rods within a certain length at the beginning of the anchorage zone (e.g. Steiger et al. 2007). Strengthening of the steel connecting profile should also be considered to prevent additional flexibility due to local buckling and plasticization of the flanges. It is also important to improve the quality of the gluing process to ensure a fully glued length of the rods, which is crucial to increase the reliability of the connections.

Acknowledgments The authors wish to acknowledge the financial support from the Lean Wood Engineering centre, from VINNOVA - The Swedish Governmental Agency for Innovation Systems, from The European Union's Structural Fund—The Regional Fund, and for all the support obtained from Moelven Töreboda, the industrial partner in the project. The experiments were conducted at Complab Laboratory at the Department of Civil, Mining and Environmental Engineering at Luleå University of Technology in Sweden. The employees/technicians of Complab Laboratory are gratefully acknowledged for all their invaluable and professional input. The contribution made by Prof. Ulf Arne Girhammar to the analytical part of this manuscript is also gratefully acknowledged.

References

Aicher S, Gustafsson PJ, Wolf M (1999) Load displacement and bond strength of glued-in rods in timber influenced by adhesive, wood density, rod slenderness and diameter. In: International RILEM Symposium on Timber Engineering, Stockholm, Sweden

Baroth J, Bode L, Bressolette P, Fournely E, Racher P (2004) Glued-in rod connections in bending: experiment and stochastic finite-element modelling. 8th World Conference on Timber Engineering, Lahti, Finland

Batchelar M (2006) Timber frame moment joints with glued-in steel rods—a designer's perspective. In: 9th World Conference on Timber Engineering, Portland, Oregon, USA

BKR (1998) Design regulations BKR—mandatory provisions and general recommendations BFS 1993:58 with amendments up to BFS 1998:39 (in Swedish), Boverket, Karlskrona

Carling O (2001) Glulam handbook. Svensk Limträ AB, Stockholm (in Swedish)

DIN 1052:2008-12 Entwurf (2008) Berechnung und Bemessung von Holzbauwerken—Allgemeine Bemessungsregeln und Bemessungsregeln für den Hochbau. DIN, Berlin, Germany

EN 1194 (1999) Timber structures—Glued laminated timber—strength classes and determination of characteristic values. European Committee for Standardisation, Brussels, Belgium

EN 1993-1-1 (2005) Eurocode 3: Design of steel structures—Part 1-1: General rules and rules for buildings. European Committee for Standardisation, Brussels, Belgium

EN 1995-1-1 (2004) Eurocode 5: design of timber structures—part 1-1: general—common rules and rules for buildings. European Committee for Standardisation, Brussels, Belgium

Filiatrault A, Foschi R (1991) Static and dynamic tests of timber shear walls fastened with nails and wood adhesives. Can J Civ Eng 18(5):749–755

Fragiacomo M, Batchelar M (2012) Timber frame moment joints with glued-in steel rods. Part 1: design. J Struct Eng ASCE 138(6):789–801

Gattesco N, Gubana A (2006) Performance of glued-in joints of timber members. In: 9th World Conference on Timber Engineering, Portland, Oregon, USA

ISO 3130 (1975) Wood—determination of moisture content for physical and mechanical tests. International Organization for Standardization

ISO 3131 (1975) Wood—determination of density for physical and mechanical tests. International Organization for Standardization

Källsner B, Girhammar UA (2008) Horizontal stabilising of light frame timber structures. Plastic design of wood-framed shear walls. SP Technical Research Institute of Sweden, p 47 (in Swedish)

Salenikovich AJ, Dolan JD (2003) The racking performance of shear walls with various aspect ratios. Part I. Monotonic tests of fully anchored walls. For Prod J 53(10):65–73

Serrano E (2001) Glued-in rods for timber structures—an experimental study of softening behaviour. Mater Struct J 34(4):228–234

Sousa HS, Branco JM, Lorenco PB (2013) Glulam mechanical characterization. Mater Sci Forum 730–732:994–999

Steiger R, Gehri E, Widmann R (2007) Pull-out strength of axially loaded steel rods bonded in glulam parallel to the grain. Mater Struct 40(1):69–78

Tlustochowicz G (2010) Racking behaviour of stabilising walls and the anchorage systems for beam and post system in timber: Test report, Luleå University of Technology, Luleå, Sweden

Tlustochowicz G (2011) Stabilising system for multi-storey beam and post timber buildings. Doctoral thesis, Luleå University of Technology, Luleå

Tlustochowicz G, Johnsson H, Girhammar UA (2010a) Beam and post system for non-residential multi-storey timber buildings—horizontal displacements in stabilising system. In: 11th world conference on timber engineering, Riva del Garda, Italy

Tlustochowicz G, Kermani A, Johnsson H (2010b) Beam and post system for non-residential multi-storey timber buildings—conceptual framework and key issues. In: 11th world conference on timber engineering, Riva del Garda, Italy

Typgodkännandebevis 1396/78 (2009) Screw glued into glued laminated timber (in Swedish), SP Sveriges Tekniska Institut, SP SITAC, Karlskrona, Sweden

Vessby J (2008) Shear walls for multi-storey timber buildings. Licentiate thesis, School of Technology and Design Växjö University, Växjö, Sweden